

CONSTRUCTION OF PARALLEL COUPLING MODEL AND CONTROL STRATEGY FOR LED WELDING TRANSMISSION SYSTEM

MEI Yang-han^{1,2}, PENG Yan^{1,*}, HU Zong-hui³, ZUO Da-li^{1,2}

Aiming at the low transfer efficiency of traditional LED bracket welding, Problems such as poor transfer coordination and low synchronization accuracy caused by external interference of dual-axis platform, a synchronous control strategy with disturbance compensation is analyzed and designed. The model is established based on software of MATLAB. Finally, the test experiment was carried out on the prototype. The results show that the parallel deviation coupling synchronization control with disturbance compensation is better than the traditional control strategy, synchronous control error is reduced by 60%, and tracking error is reduced by 45%. The disturbance immunity and stability of the system are obviously enhanced, the tracking and synchronization error are both reduced, It also provides a more powerful basis for industrial automation applications.

Keywords: Motor Control; Screw Drive; Coupling Control; Simulation Model

1. Introduction

In the modern electronic equipment industry, automatic welding equipment has been widely used, such as LED automatic welding wire, circuit board welding and electronic circuit welding. The automatic welding equipment is a complex multi-axis coordinated working system. The key factor in quality is the simultaneous control of multiple axes, which affects welding precision, efficiency and packaging. Taking the LED automatic welding equipment as an example, the welding process needs to meet the two matching times and speeds, that is the time for the feeding shaft to complete the unit welding length, the time for the feeding shaft to complete the single feeding, and the time for the loading shaft to rotate for one cycle are equal, and the speed is matched, At the intersection, the dispensing speed of the dispensing shaft is equal to the feeding speed of the welding. As a wide-ranging problem, multi-axis synchronous control not only exists in welding machinery, but also involves all aspects of automation control. Therefore, multi-axis synchronous control technology has received extensive attention and

¹ Lecturer, DongGuan Polytechnic, Dongguan , 523808, China;

² Guangdong Textile Industry Intelligent Testing Technology Research Center, Dongguan, 523808, China;

³ Engineer, Shenzhen Yuhui Photoelectric Technology Co., Ltd., Shenzhen, 518052, China.

* Correspondence author: Peng Yan .e-mail:969480854@qq.com

engineering practice research by experts and scholars at home and abroad [1, 2, 3].

At present, with the wide application of the two-axis synchronous control system in electromechanical automation equipment, two main synchronous control modes of mechanical and electronic control are formed. The mechanical synchronization control is simple, but the structure is complicated, which leads to many transmission errors, the result is that the control precision is very low. The electronic control synchronous control does not have these shortcomings. Therefore, the electronically controlled synchronous control mode has become the mainstream direction of the development of the dual-axis synchronous control mode. The electronically controlled synchronous control mode mainly has three structural forms: master-slave control, parallel control and cross-coupling control [4, 5]. The synchronous coupling control mode refers to a control method that uses the compensation unit to compensate the deviation of the two axes on the basis of the parallel control mode. The compensation unit compensates the two axes based on the acquisition of the two-axis deviation signal, and obtains better synchronization control effect [6, 7, 8]. In view of the advantages of coupling control, this paper constructs a position control method based on deviation coupling. And carry out simulation verification analysis.

2. Integral Design of LED Welding Feed System

The whole process of LED bracket welding and assembly is as follows: take the LED bracket, load, weld, unload, sub-package, and finally into the warehouse. The main function of this automated dispensing equipment is to fully automate the above process. That is, the device can automatically take the LED bracket and push it into the material transfer rail, transfer it to the designated position, complete the welding, then transfer it to the position of the empty magazine, complete the boxing work, and finally push into the small warehouse. Complete a welding cycle, the specific welding process is shown in Fig.1.

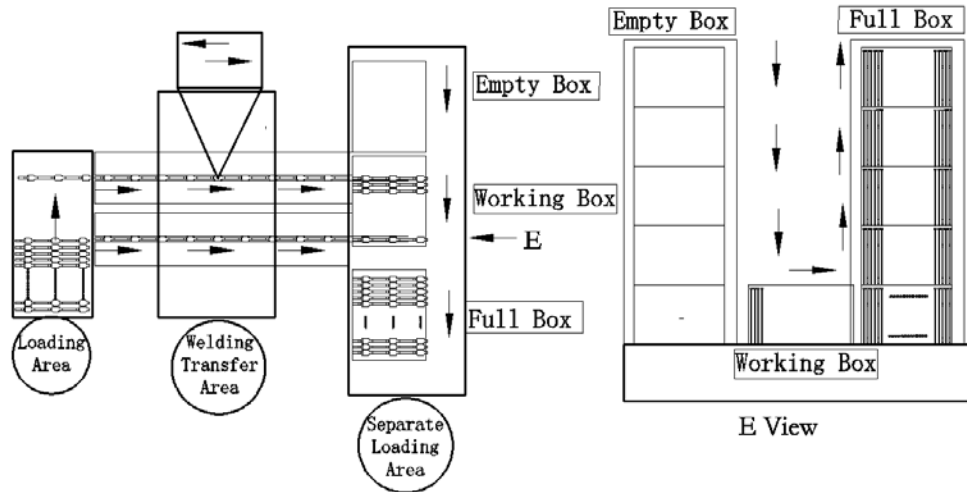


Fig .1. Double-track stereo sub-assembly scheme

According to the welding process, in order to achieve high-efficiency welding and dispensing, the two-way feed servo shafts are fed separately. However, if the two axes are fed separately, the positioning control algorithm of spindle motor will be more complicated, and frequent positioning takes more time. Moreover, the motor is frequently moved to increase the load, which leads to an increase in the design cost of the spindle. Therefore, in order to improve the efficiency, the control precision and reduce the cost, the synchronous control design of the two-way feed servo axis is adopted, and the design of the two-way feed structure is as shown in Fig.2. It is mainly used to transport LED simultaneously with two motors-two tracks. The key to this design is synchronous feed servo control, which ensures synchronization of feed welding control, high-speed and high-precision positioning welding, and guarantees the quality of LED product welding.

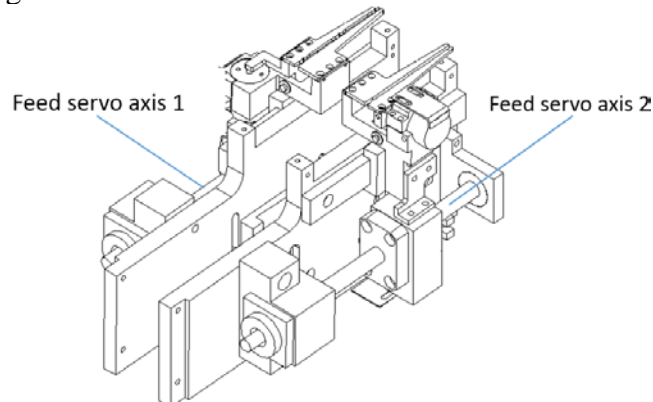


Fig. 2. Dual-track Servo Feed Structure

3. Construction Feed System Simulation Model

The complete model establishment of the two-way dual-motor synchronous feed system should include a full-closed mathematical model from the controller end to the final workbench. For the convenience of establishment modeling, it is divided into two parts to be modeled separately. The boundary line is to establish the mechanical dynamics model of the motor-ball screw-workbench and the electronic control mathematical model of the controller-motor.

3.1 Construction of Single Feed Model

In order to realize the two-way synchronous control, the construction of the single-channel control model must be completed. According to the design structure of Fig.2. the model is simplified as necessary, which is simplified to the motor-ball screw-workbench diagram shown in Fig. 3. Its main parts include: motor, coupling, ball screw and workbench, where reduction ratio is 1:1 (no gear reducer), the modeling process is as follows:

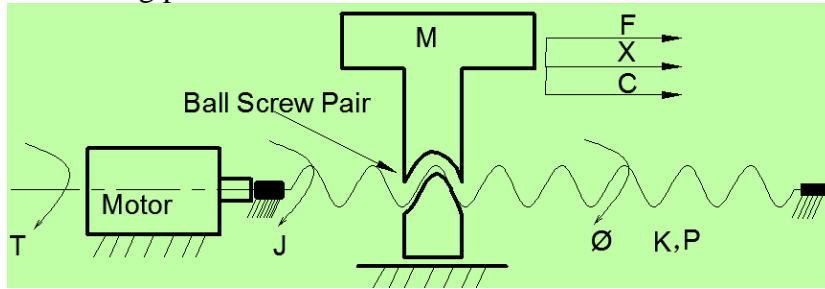


Fig. 3. Single-screw servo feed system model

The mechanical transmission dynamics model of the ball screw drive is established by the principle of Jean le Rond d' Alembert [9, 10, 11] :

$$T = \left(\frac{2\pi}{P} \cdot J_0 + M \cdot \frac{P}{2\pi} \right) \ddot{X}(t) + C \cdot \frac{P}{2\pi} \dot{X}(t) \quad (1)$$

Where: T is the torque on the screw rod, P is the lead of the screw, M is the mass of the table, J_0 is the moment of inertia of the screw, C is damping coefficient of the system, and $X(t)$ is the displacement of the workbench.

From the torque balance equation, the torque conversion of the screw drive is converted to the motor shaft, so the torque balance equation on the motor shaft can be obtained:

$$K[\dot{\theta}(t) - \frac{2\pi}{P} X(t)] = T + J_1 \cdot \frac{2\pi}{P} \ddot{X}(t) \quad (2)$$

Where: K is the torsion stiffness of the screw, $\dot{\theta}(t)$ is the amount of rotation of the motor, J_1 is the moment of inertia of the motor.

In combination with the screw and motor drive model above, the eq.(1) is substituted into the eq. (2) to obtain:

$$K \cdot \dot{\phi}(t) = K \frac{2\pi}{P} X(t) + C \cdot \frac{P}{2\pi} \dot{X}(t) + (J_1 \frac{2\pi}{P} + J_0 \frac{2\pi}{P} + M \cdot \frac{P}{2\pi}) \ddot{X}(t) \quad (3)$$

Where: the input $\dot{\phi}(t)$ is the amount of rotation of the motor, and the output $X(t)$ is the platform displacement.

Thus the open loop transfer function can be pushed to eq.(4).

$$G_1(S) = \frac{X(S)}{\dot{\phi}(S)} = \frac{K}{(J_1 \frac{2\pi}{P} + J_0 \frac{2\pi}{P} + M \cdot \frac{P}{2\pi}) S^2 + C \cdot \frac{P}{2\pi} S + K \frac{2\pi}{P}} \quad (4)$$

After calculating the selected screw and motor model, it is calculated that $J_1 = 0.045 * 10^{-4} kg \cdot m^2$, $J_0 = 8.738 * 10^{-6} kg \cdot m^2$ and the screw pitch $P = 0.005m$, the damping coefficient (C) of the screw platform under the lubricating oil system is 0.469, and the torsional stiffness (K) is =0.82.

Therefore, the controlled object model can be simplified to eq. (5).

$$G_1(S) = \frac{X(S)}{\dot{\phi}(S)} = \frac{4.1 \times 10^{-3}}{0.00028S^2 + 0.363S + 1} \quad (5)$$

3.2 Construction of Motor Control Model

At present, the permanent magnet synchronous motor and the brushless DC motor are widely used in the servo feed control of electromechanical products. Combined with the characteristics of small torque required in the process of LED bracket transfer, the design uses a permanent magnet synchronous motor.

The stator voltage equation of the permanent magnet synchronous motor in the d-q coordinate system is eq. (6) [12]:

$$\begin{cases} u_d = R_s i_d + \dot{\psi}_d - \psi_q \omega_r \\ u_q = R_s i_q + \dot{\psi}_q + \psi_d \omega_r \end{cases} \quad (6)$$

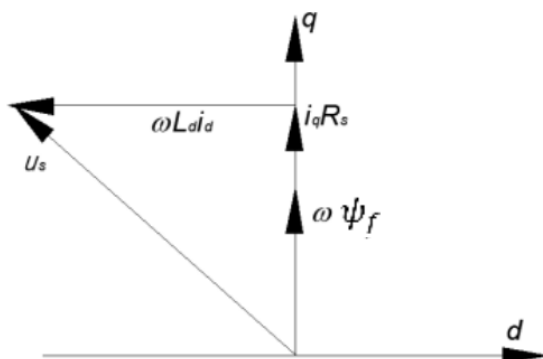


Fig.4. State motor vector in $i_d = 0$

The stator flux linkage equation is eq. (7):

$$\begin{cases} \psi_d = L_d i_d + \psi_f \\ \psi_q = L_q i_q \end{cases} \quad (7)$$

The electromagnetic torque equation is eq. (8):

$$T_e = 1.5P[\psi_f i_q + (L_d - L_q)i_d i_q] \quad (8)$$

The mechanical equation of motion of a permanent magnet synchronous motor is eq. (9):

$$T_e = J_1 \frac{d\omega_r}{dt} + T_d + C_d \omega_r \quad (9)$$

Where u_d , u_q -the mover voltages on the d -q axes;

i_d , i_q -the mover currents on the d- q axes;

ψ_d , ψ_q - the permanent magnet flux linkage on the d-q axis;

L_d , L_q -are for the mover inductance on the d-q axis;

ψ_f - the magnetic flux of the rotor of the motor;

R_s - the stator winding resistance;

T_e -electromagnetic torque for the motor;

T_d -for the motor load resistance torque;

J_1 - for the motor's moment of inertia;

ω_r - motor mechanical angular velocity;

C_d - is the motor damping coefficient.

From the mathematical model of the synchronous motor, it can be concluded that the control of the motor output torque ultimately comes down to the control of the motor's straight and quadrature axes. The most common current control method for permanent magnet synchronous motor is $i_d = 0$, which is to make the stator current vector and the permanent magnet magnetic orthogonal in space. The method is simple and the workload is small, and the application is extensive. Therefore, at that time of $i_d = 0$, the motor torque equation can be transformed into eq. (10).

$$T_e = 1.5P\psi_f i_q \quad (10)$$

Therefore, on the q-axis, the stator voltage equation is further simplified to eq. (11) (without considering the effect of the armature response on the output torque).

$$R_s i_q + L_s \frac{di_q}{dt} = u_q - \psi_d \omega_r \quad (11)$$

Where ω_n ($\omega_r = \omega_n \cdot P_n$) is the mechanical angular frequency of the rotor of motor, and P_n is logarithm of magnetic poles.

Eq. (12) derived from of laplacian variation eqs. (11).

$$\frac{I(S)}{U(S) - \psi_d \omega_n \cdot P_n(S)} = \frac{1}{L_s S + R_s} \quad (12)$$

Eq. (13) derived from of laplacian variation eqs. (10).

$$\frac{\omega_n(s)}{1.5P\psi_f I_q(s) - T_d(s)} = \frac{1}{J_1 s + C} \quad (13)$$

The mathematical model of the motor armature can be obtained as a first-order inertia link, and the transfer function block diagram design is shown in Fig.5, where $K_f = \psi_d P_n$ is the back electromotive force and $K_L = 1.5P\psi_f$ is the torque coefficient.

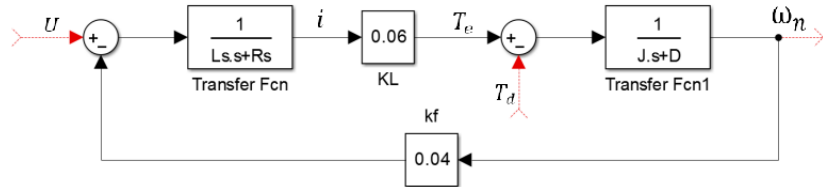


Fig. 5. The model block diagram of motor armature

Only the middle-loop speed loop and the inner-loop current loop are considered when establishing the mathematical model of controller-motor. Because the speed loop cross-angle frequency is low, the current loop can be simplified to the first-order inertia link. In order to make the system have good anti-interference performance and achieve no static difference of the speed, the speed loop can be corrected to a typical type II system [13,14].

Combined with the control requirements of subsequent dual motor synchronization, the speed loop should have better Speed following characteristics and anti-interference ability, and the position ring should have greater rigidity, thus strictly ensuring positional accuracy. Thus, fine-tune the parameters of each controller and build a system simulation model in the environment of simulink as shown in Fig.6.

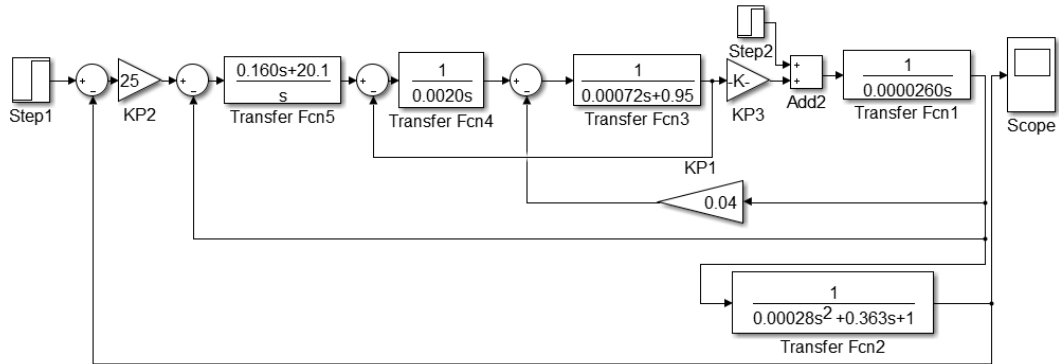


Fig.6. Integrated control model of single-circuit motor system

For the control mode system, input a step signal with a response time of 2s and an amplitude of 1 and load an interference signal with a delay of 3s. Observe the step response of the system as shown in Fig.7.

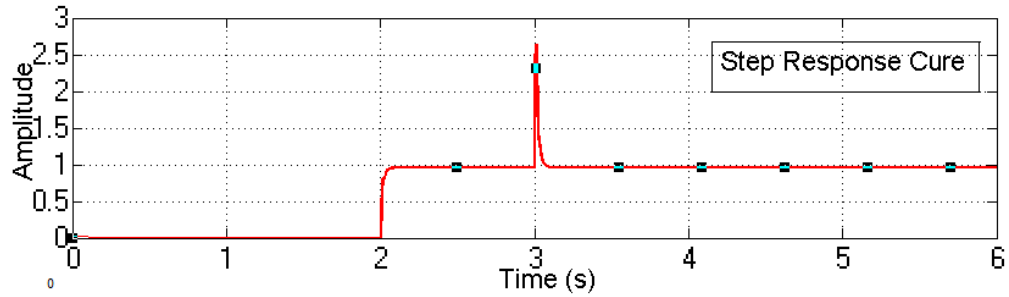


Fig. 7. Step response curve of single-circuit motor system

It can be seen from the simulation results that the system recovers its original state quickly after being disturbed, and the stability of the system is well controlled. However, the amplification response shows that the system response time is about 0.12 s, the jitter amplitude is large. The state error reaches 6%, and the positioning accuracy of the system is greatly disturbed. This will not meet the design requirements for accurate positioning of the LED bracket. In order to improve the tracking control accuracy of servo system, the position control is improved (as shown in Fig. 8). The position loop regulator is added to the system (as shown in Fig.9). The relatively appropriate proportion, integral and differential coefficients are determined through experimental debugging.

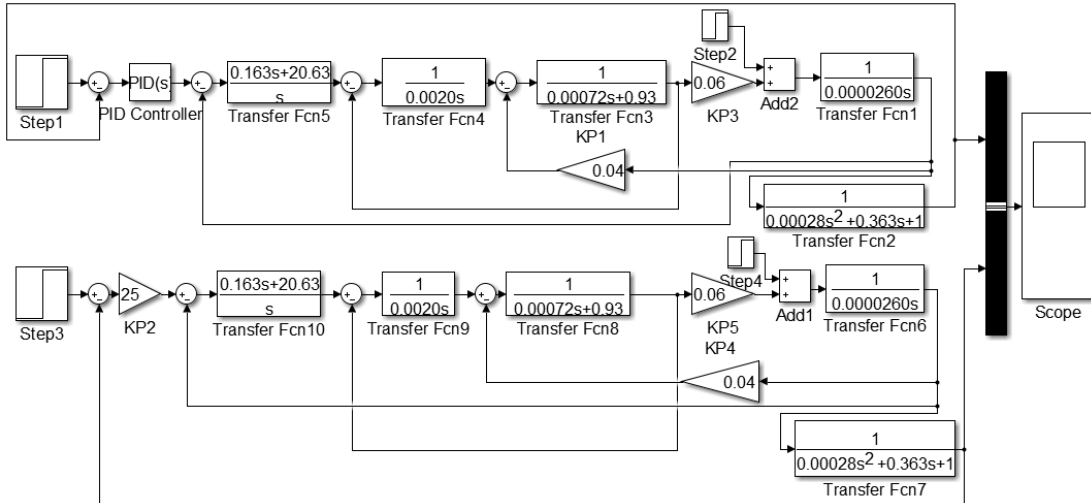


Fig.8. Two-way control model of dual motor

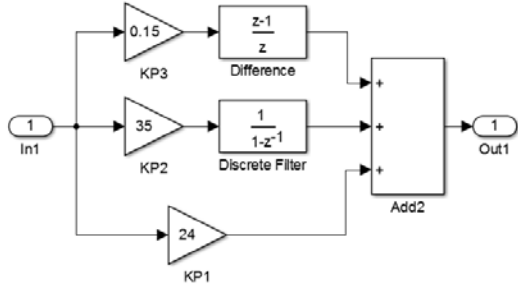


Fig.9. Controller model of position adjustment

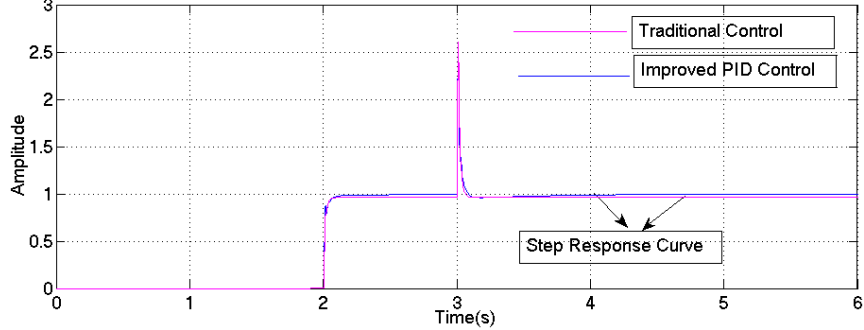


Fig.10. Step response comparison of traditional-improved control

The simulation results show that with the improved PID control method, the jitter error of the step response is significantly reduced, and the steady-state error is reduced to 0.8%, which achieves better response and robustness, which lays a solid foundation for the subsequent construction of the two-way control model.

3.3 Two-way Synchronous Coupling Control Model

In order to realize the synchronous control of the two-way servo system and ensure the tracking and synchronization of the two-way screw drive tables during operation, the design is based on the deviation coupling control, which consists of two parts. Part of it is the position error calculation model, and the other part is the error redistribution module [15]. Specifically, the position error calculation model calculates the system out-of-synchronization error, and compensates the system error separately through the redistribution module, solving the imbalance force between the screw, the guide rail and the transfer workbench, and affecting the synchronous feed, which affect synchronization feed accuracy.

For the two-motor servo control system, define the position tracking error of the single axis system as eq.(14).

$$\varepsilon_i = X_o - X_i \quad (14)$$

Where X_o is target position, and X_i is the actual arrival position, as shown in

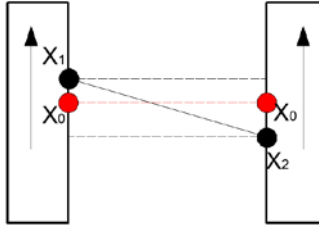


Fig. 11. Schematic diagram of two-axis synchronous control

According to the requirement of synchronization control, the synchronization error of two axes is defined as eq. (15).

$$\begin{cases} \Delta_1 = \varepsilon_1 - \varepsilon_2 \\ \Delta_2 = \varepsilon_2 - \varepsilon_1 \end{cases} \quad (15)$$

Where Δ_1 and Δ_2 are the synchronization error of X_1 and X_2 axes, when the synchronization error are zero, two axes are synchronous motion, and expressed in matrix form as eq. (16).

$$\Xi = A\epsilon \quad (16)$$

$$\text{Where } \Xi = [\Delta_1, \Delta_2]^T, \epsilon = [\varepsilon_1, \varepsilon_2]^T, A = \begin{bmatrix} 1 & -1 \\ -1 & 1 \end{bmatrix}$$

In order to make the two-axis moving target position of the feed system consistent, it is necessary to reduce the tracking error and the synchronization error at the same time. Therefore, the two errors are combined to define the integrated error as eq.(17).

$$\epsilon_Z = [\varepsilon_1, \varepsilon_2]^T + \alpha [\varepsilon_1 - \varepsilon_2, \varepsilon_2 - \varepsilon_1]^T = \epsilon + \alpha \Xi \quad (17)$$

Substituting eq.(17) into equation.(16).

$$\epsilon_Z = \epsilon + \alpha \Xi = (E + \alpha A) \epsilon \quad (18)$$

Where α is the coupling coefficient of the two motor control, E is an identity matrix, $E + \alpha A$ is a positive definite matrix. From eq. (18) can be concluded, only $\epsilon \rightarrow 0$, just $\epsilon_Z \rightarrow 0$ (That is $\Xi \rightarrow 0$: the controller target is to ensure that both the synchronization error and the tracking error are reduced).

In order to achieve the above objectives, the deviation coupling control strategy is adopted in this paper. as shown in Fig.12. where $\epsilon = E_{x1}C_{x1} - E_{x2}C_{x2}$ and the PID module together form the error, C_{x1} and C_{x2} are the error redistribution module, to achieve separate compensation for the synchronization error. According to the selected value of C_{x1} and C_{x2} (which can be a constant or a function), get different ways of error redistribution, which effectively realizes the closed-loop control of position error.

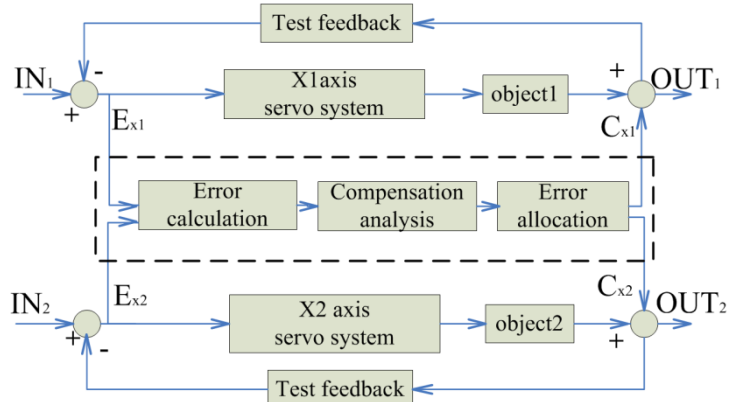


Fig. 12. Cross-coupling controller model

The two-way system is simulated and modeled by the deviation coupling control method. The Simulink model is shown in Fig.13. It is ideally considered that the two-axis mathematical model is completely consistent, and the subsystem PID regulator is also completely consistent. When the same disturbance is added, the system simulation results that the two-axis displacement is completely the same. Under the actual mechanical conditions, the disturbance of the two axes is not completely the same. Therefore, in the simulation, the disturbance signals of different intensities need to be added to the two axes. When different disturbances are added to the two axes (the amplitude of the X1 axis is 2 and the X2 axis is 5), the simulation results are shown in Fig. 14. The simulation results show that the synchronization error of the system is obviously less, which is 60% lower than that of the traditional control method, and the following error is reduced by 45%, and achieve the desired effect.

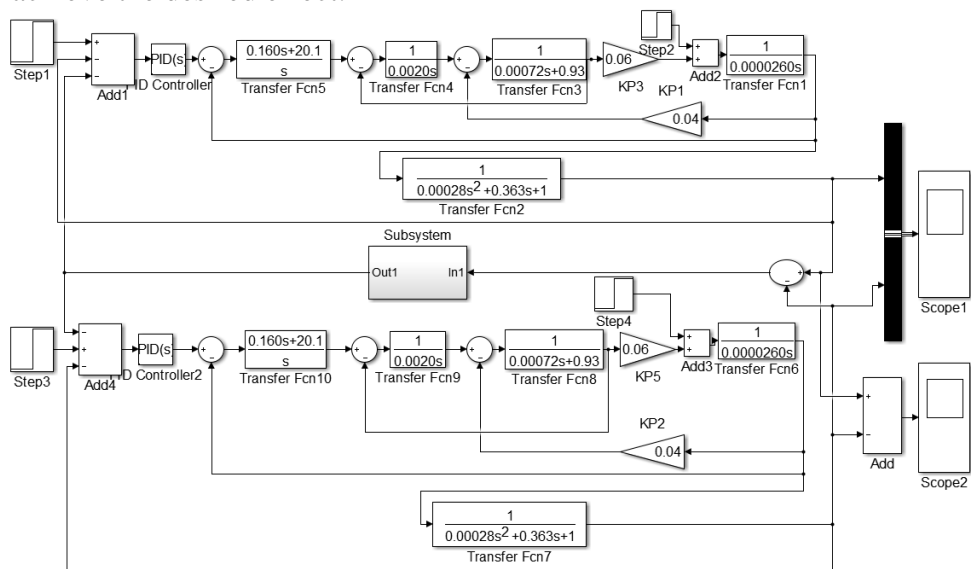


Fig.13. Model of Synchronous coupling control

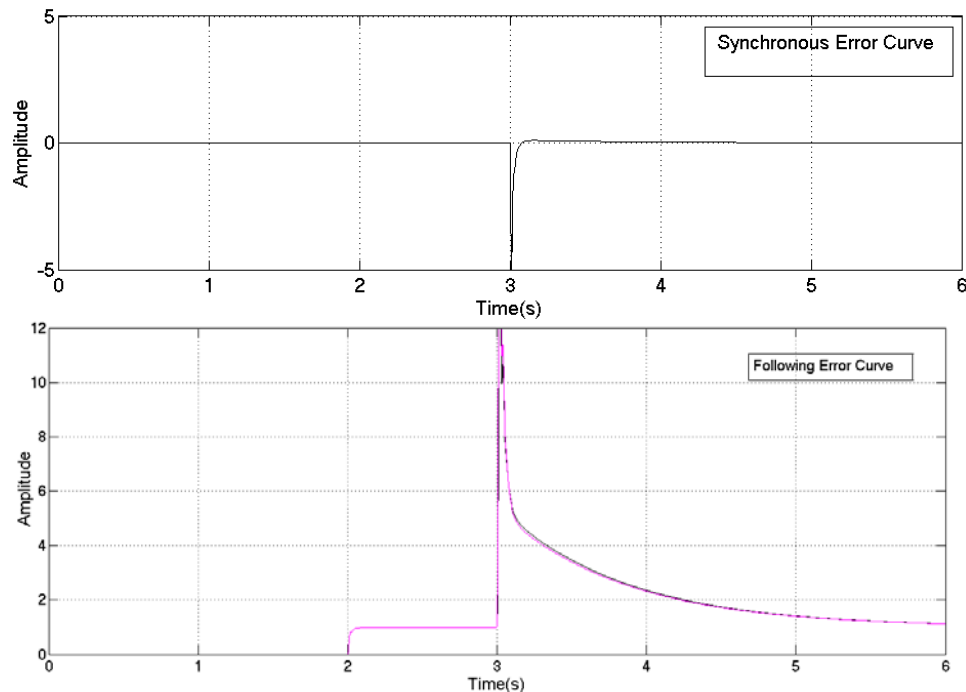


Fig. 14. Curve graph of synchronization and following error

4. Verification analysis

In order to verify the effectiveness and practicability of the control strategy, according to the product design requirements, the prototype is coupled to the synchronous control test, so that the feed servo motor moves with the S acceleration and deceleration curve, and the screw platform reciprocates on the guide rail before and after the improved control. The position of the platform is detected. The actual experimental data is shown in Fig.15. After the deviation coupling is used for synchronous control, the relative deviation of the platform is reduced by 50%.

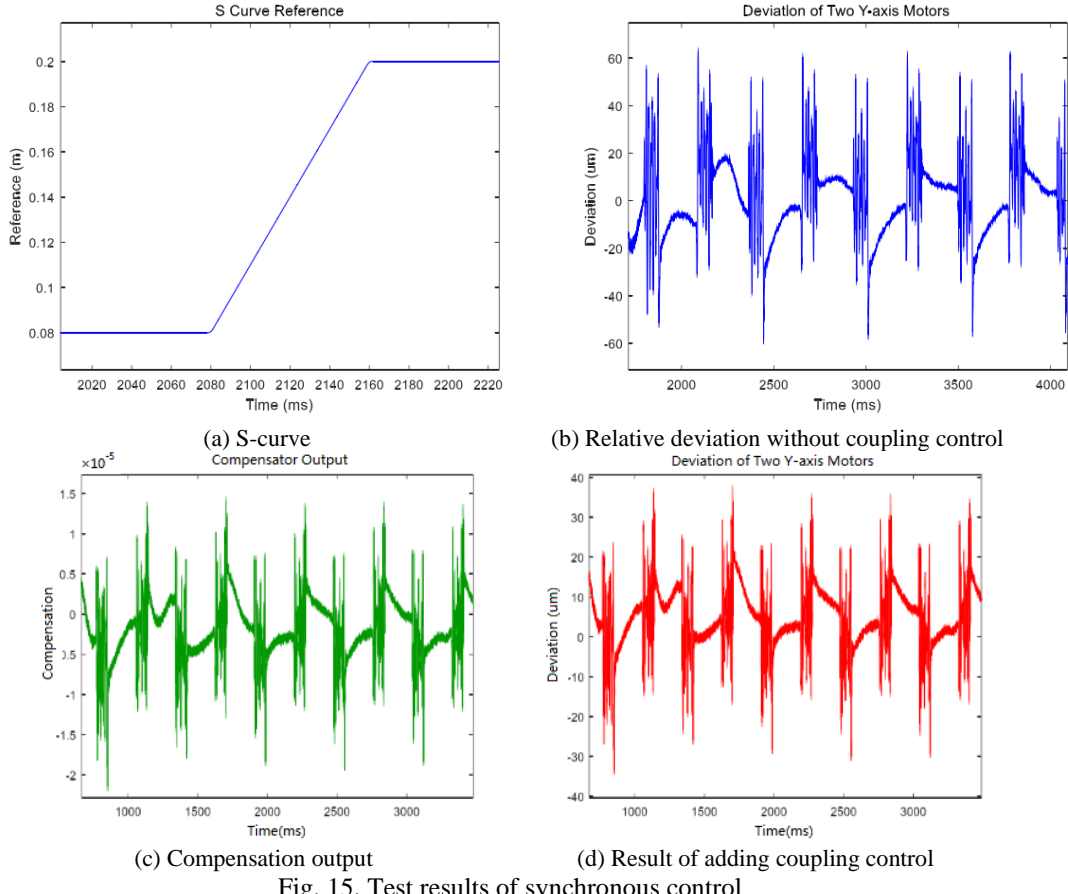


Fig. 15. Test results of synchronous control

5. Conclusion

Based on the research of the control method of the two-way feed servo system, the mathematical model of the two-way transfer system was established. The parallel deviation coupling control strategy was proposed. The simulation model was built with Matlab and the prototype was tested. Comparison simulation and test data show that the relative deviation of the platform was reduced by 50%. Compared with the traditional control method, the deviation coupling control method is reduced by 60%, and the follow-up error is reduced by 45%, which provides a reliable research method for the subsequent multi-channel synchronous control scheme design, and also provides a reference basis for the development and design of automatic products and system parameter setting.

Acknowledgments

The authors would like to acknowledge Project (Project Number: 2017GkQNCX117) Supported by 2017 scientific research Project of Department

of Education of Guangdong Province, China. Project Name: Research on key technology development of Transfer and Packaging System for LED Bracket.

R E F E R E N C E S

- [1]. *J.D. Wang, Z.J. Zhang, C.X. Liang, et al.* Research and Application of Electronic CAM Key Technology in Packaging Machine. *Packaging Engineering*, **vol. 34**, no. 7, 2013, pp. 48-51.
- [2]. *T. Choi, H. Do, D. Park, C. Park, J. Kyung.* Real-time synchronisation method in multi-robot system. *Electronics Letters*, **vol. 50**, no. 24, 2014, pp. 1824–1826.
- [3]. *M.R. Soltanpour, M.H. Khooban, M.R. Khalghani.* An optimal and intelligent control strategy for a class of nonlinear systems:adaptive fuzzy sliding mode. *Journal of Vibration&Control*, **vol. 8**, no. 8, 2014, pp. 10-11.
- [4]. *L.H. Sheng, L.M. Hou, T.C. Li, D. Lin.* Research on Speed Synchronization of High Performance Control System for double permanent magnet synchronous motor. *Measurement & Control Technology*, **vol. 37**, no. 9, 2018, pp. 131-135+140.
- [5]. *R.Q. Zhang, J.X. Hu.* Motor Synchronous Control Experimental Study Based on Deviation Coupling Control. *Modular Machine Tool & Automatic Manufacturing Technique*, no. 2, 2018, pp. 100-104.
- [6]. *M.Y. Dong, H. Qing, Z. Fei.* Synchronous motion control of biaxial driving system with-linear servo motors, Shenyang: International conference on automation and logistics, 2009, pp. 638-641.
- [7]. *S.Y. Cheng, W.J. Ji, Z.J. Wang.* The Cross-coupled Synchronous Control of Multi- Servo Motors Based on Fuzzy-PID. *Journal of Beijing In-stitute of Petro-chemical Technology*, **vol. 22**, no. 4, 2014, pp. 54-57.
- [8]. *J.R. Conway, C.A. Ernesto, R.T. Farouki, et al.* Performance analysis of cross-coupled controllers for CNC machines based upon precise real-time control error measurement. *International Journal of Machine Tools and Manufacture*, **vol. 52**, no. 1, 2012, pp. 30-39.
- [9]. *W.Y. Cheng, L. Luo, Z.G. Liu.* Improvement Study of Deviation Coupling Compensation Backstepping Synchronous Control Arithmetic. *Machinery Design & Manufacture*, no. 2, 2016, pp. 41-44+48.
- [10]. *H. Li, D.C. Wang, H. Zhang.* Synchronization Control Based on Cross-Coupling Technology CNC Machine Tools Biaxial Drive . *Machinery Design & Manufacture*, no. 7, 2016, pp. 130-134.
- [11]. *C. Chamroon, M.O.T. Cole, T. Wongratanaaphisan.* An active vibration control strategy to prevent nonlinearly coupled rotor-stator whirl responses in multimode rotordynamic systems. *Control Systems Technology, IEEE Transactions on*, **vol. 22**, no. 3, 2014, pp. 1122-1129.
- [12]. *Z.W. Zhang, J. Hao, H.H. Tan.* Model Reference Adaptive Control of Permanent Magnet Synchronous Motor for Packaging Printing. *Bulletin of Science and Technology*, **vol. 35**, no. 1, 2019, pp. 173-176.
- [13]. *S.T. Xie.* The Research of CNC Grinding Wheel Dressing System based on Double-drive Synchronous Feeding Technology. *Wuhan University of Technology, China*, 2015.
- [14]. *J.L. Zhang, Y.M. Zhang, J.Z. Ding, J.X. Gao.* *Journal of Shanghai Jiaotong University. Journal of Shanghai Jiaotong University*, **vol. 52**, no. 9, 2018, pp. 1023-1030.
- [15]. *H.L. Gao, Y. Sang, L.T. Shao.* Discuss on Synchronization Control and Its Typical Application. *Hydraulics Pneumatics&Seals*, **vol. 32**, no. 5, 2012, pp. 1-7.